The EMBO Journal (2010) 29, 517–531 | © 2010 European Molecular Biology Organization | All Rights Reserved 0261-4189/10
www.embojournal.org

THE EMBO JOURNAL

mNUDC is required for plus-end-directed transport of cytoplasmic dynein and dynactins by kinesin-1

Masami Yamada[1], Shiori Toba[1], Takako Takitoh[1], Yuko Yoshida[1], Daisuke Mori[1], Takeshi Nakamura[2], Atsuko H Iwane[3], Toshio Yanagida[3], Hiroshi Imai[4], Li-yuan Yu-Lee[5], Trina Schroer[6], Anthony Wynshaw-Boris[7] and Shinji Hirotsune[1,*]

[1]Department of Genetic Disease Research, Graduate School of Medicine, Osaka City University, Osaka, Japan, [2]Laboratory of Bioimaging and Cell Signaling, Graduate School of Biostudies, Kyoto University Yoshida Konoe-cho, Kyoto, Japan, [3]Laboratories for Nanobiology, Graduate School of Frontier Biosciences, Osaka University, Suita, Osaka, Japan, [4]ERATO Actin Filament Dynamics Project, Japan Science and Technology Agency, RIKEN SPring-8 Center, Sayo, Hyogo, Japan, [5]Program in Cell and Molecular Biology, Department of Medicine, Baylor College of Medicine, Houston, TX, USA, [6]Department of Biology, The Johns Hopkins University, Baltimore, MD, USA and [7]Department of Pediatrics and Institute for Human Genetics University of California, San Francisco School of Medicine, Parnassus, San Francisco, CA, USA

Lissencephaly is a devastating neurological disorder caused by defective neuronal migration. The *LIS1* (or *PAFAH1B1*) gene was identified as the gene mutated in lissencephaly patients, and was found to regulate cytoplasmic dynein function and localization. In particular, LIS1 is essential for anterograde transport of cytoplasmic dynein as a part of the cytoplasmic dynein–LIS1–microtubule complex in a kinesin-1-dependent manner. However, the underlying mechanism by which a cytoplasmic dynein–LIS1–microtubule complex binds kinesin-1 is unknown. Here, we report that mNUDC (mammalian NUDC) interacts with kinesin-1 and is required for the anterograde transport of a cytoplasmic dynein complex by kinesin-1. mNUDC is also required for anterograde transport of a dynactin-containing complex. Inhibition of mNUDC severely suppressed anterograde transport of distinct cytoplasmic dynein and dynactin complexes, whereas motility of kinesin-1 remained intact. Reconstruction experiments clearly demonstrated that mNUDC mediates the interaction of the dynein or dynactin complex with kinesin-1 and supports their transport by kinesin-1. Our findings have uncovered an essential role of mNUDC for anterograde transport of dynein and dynactin by kinesin-1.

The EMBO Journal (2010) **29,** 517–531. doi:10.1038/emboj.2009.378; Published online 17 December 2009
Subject Categories: membranes & transport
Keywords: adaptor; dynein; kinesin-1; Lis1; mNUDC

*Corresponding author. Department of Genetic Disease Research, Osaka City University, Graduate School of Medicine, Asahi-machi 1-4-3 Abeno, Osaka 545-8585, Japan. Tel.: +81 6 6645-3725; Fax: +81 6 6645 3727; E-mail: shinjih@med.osaka-cu.ac.jp

Received: 28 November 2008; accepted: 19 November 2009; published online: 17 December 2009

Introduction

Lissencephaly is a severe human neuronal migration defect characterized by a smooth cerebral surface, mental retardation and seizures (Dobyns, 1989; Dobyns *et al*, 1993). The *LIS1* gene was the first gene cloned in any organism important for neuronal migration, as it was deleted or mutated in humans with lissencephaly in a heterozygous manner (Reiner *et al*, 1993). LIS1 and its binding protein, NDEL1, regulate cytoplasmic dynein (Niethammer *et al*, 2000; Sasaki *et al*, 2000; Gupta *et al*, 2002; Wynshaw-Boris, 2007). We recently reported that LIS1 and NDEL1 cooperatively regulate anterograde transport of cytoplasmic dynein in a kinesin-dependent manner (Yamada *et al*, 2008). In addition, NDEL1 also regulates microtubule organization with Aurora-A, which is essential for neurite extension (Mori *et al*, 2009). Interestingly, half of LIS1 is degraded through calpain-dependent proteolysis, and that inhibition or knockdown of calpains protects LIS1 from proteolysis, which leads to the rescue of the phenotypes in *Lis1*$^{+/-}$ mouse (Yamada *et al*, 2009).

Accumulating evidence has uncovered an evolutionarily conserved pathway that involves LIS1 and cytoplasmic dynein (Morris *et al*, 1998a; Efimov and Morris, 2000; Han *et al*, 2001; Vallee *et al*, 2001; Vallee and Tsai, 2006; Wynshaw-Boris, 2007; Zhuang *et al*, 2007). *Aspergillus nidulans* and other filamentous fungi produce long linear mycelia through which the nuclei migrate in a regular, ordered manner. Genetic analysis of fungi displaying defective nuclei migration led to the identification of a large number of proteins involved in this process (Xiang *et al*, 1995; Morris *et al*, 1998a; Minke *et al*, 1999; Efimov and Morris, 2000). For example, mutations of *nudA* (cytoplasmic dynein heavy chain) and other subunits of the dynein complex, including *nudC* (mammalian *NudC*, *mNudC*), *nudE* (*Ndel1* and *Nde1*) and *nudF* (*Lis1*), inhibit nuclear migration. Among the nud gene family, NUDC has been implicated in the regulation of dynein-mediated nuclear migration, suggesting that NUDC has a role in translocation of nuclei in proliferating neuronal progenitors as well as in migrating neurons, similar to the conserved mechanism of nuclear movement displayed by other members of the nud family in *A. nidulans*, as well as during neuronal migration in the developing mammalian brain (Morris *et al*, 1998a; Aumais *et al*, 2001, 2003). Despite extensive characterization of the relationship in the nud gene family, information of an mNUDC role in the regulation of motor proteins remains poorly understood.

Here, we report that mNUDC is an essential molecule for the anterograde transport of cytoplasmic dynein and dynactins. We demonstrated that mNUDC co-migrated with cytoplasmic dynein, dynactins and kinesin-1. Inhibition of mNUDC by a blocking antibody against mNUDC severely perturbed anterograde transport of cytoplasmic dynein and dynactins, whereas kinesin-1 movement remained intact. Depletion of mNUDC by siRNA affected subcellular

distribution of cytoplasmic dynein and dynactins. *In vitro* motility assays using purified kinesin-1 and recombinant mNUDC revealed that mNUDC supports transport of microtubules and dynactins by kinesin-1. Our data suggest that mNUDC mediates the binding of cargo molecules with kinesin-1, which is required for the anterograde transport of a cytoplasmic dynein complex and a separate dynactin complex.

Results

mNUDC co-migrates with kinesin-1 and cytoplasmic dynein and dynactins

To address the function of a mammalian homologue of NudC (mNudC), we monitored the dynamics of mNUDC fluorescence recovery after photobleaching (FRAP) using dorsal root ganglia (DRG) neurons (Yamada *et al*, 2008). We expressed GFP–mNUDC in DRG neurons and traced the movement of GFP–mNUDC by FRAP. Interestingly, mNUDC was almost exclusively transported in an anterograde manner (Figure 1A, Supplementary Figure S1B), suggesting that mNUDC was degraded after anterograde transport to the nerve terminals by the plus-end-directed motor kinesin. We recently demonstrated that LIS1 is essential for the anterograde transport of cytoplasmic dynein as a part of the cytoplasmic dynein–LIS1–tMT complex in a kinesin-dependent manner (Yamada *et al*, 2008). We hypothesized that mNUDC might be required to mediate the connection between this cytoplasmic dynein–LIS1–tMT complex and kinesin-1. To address this possibility, we first examined the co-migration of mCherry–mNUDC with GFP–kinesin light chain-1 (GFP–KLC-1) using confocal microscopy (Supplementary Figure S1C). We observed that during anterograde transport, mCherry–mNUDC co-migrated with GFP–KLC-1 (Figure 1B, Supplementary Movie 1). We also measured the frequency of co-migration, and observed that they were commonly co-migrating (Figure 1G: KLC-1/mNUDC, 79%), suggesting that mNUDC is frequently present in a kinesin-1 complex. We next examined the co-migration and frequency of co-migration of GFP–TUBB3 and GFP–dynein intermediate chain-1 (GFP–DIC1) with mCherry–mNUDC, and found highly frequent co-migration of these two proteins during anterograde transport (Figure 1C, D and G, Supplementary Movie 2 and 3: TUBB3/mNUDC, 60%; DIC1/mNUDC, 63%). These observations suggest that mNUDC is co-localized with a tMT–LIS1–cytoplasmic dynein complex during antergrade transport by kinesin-1.

Dynactin is a multisubunit protein complex, which is required for most, if not all, types of cytoplasmic dynein activity in eukaryotes. Dynactin binds dynein directly and allows the motor to traverse the microtubule lattice over long distances. A single dynactin subunit, $P150^{Glued}$, is sufficient for both activities, yet dynactin contains several other subunits that are organized into an elaborate structure. It is currently believed that the bulk of the dynactin structure participates in interactions with a wide range of cellular structures, many of which are cargoes of the dynein motor (Schroer, 2004). $P150^{Glued}$ and dynamitin, P50, are the most highly characterized dynactin proteins. We therefore addressed whether mNUDC is involved in the transport of $P150^{Glued}$ and dynamitin. FRAP analysis revealed that GFP–$P150^{Glued}$ and GFP–dynamitin were transported in both directions in the DRG (Supplementary Figure S1D and E, and 3A and B). We also examined co-migration of $P150^{Glued}$ and dynamitin with mNUDC, and found highly frequent co-migration of these proteins during anterograde transport (Figure 1E–G, Supplementary Movie 4 and 5: $P150^{Glued}$/mNUDC, 47%; dynamitin/mNUDC, 47%). These observations suggest that mNUDC is not only a component of a tMT–LIS1–cytoplasmic dynein complex, but it is also co-localized with dynactins during anterograde transport by kinesin-1.

mNUDC directly binds kinesin-1

To determine whether mNUDC can bind kinesin-1, we performed an immunoprecipitation assay. Mouse brain lysates were subjected to immunoprecipitation. Endogenous mNUDC was efficiently precipitated by an anti-mNUDC antibody (Figure 2A), along with KHC, DIC and $P150^{Glued}$, but these proteins were not precipitated with the control serum (Figure 2A). Inversely, we performed an immunoprecipitation assay using an anti-KHC antibody (Figure 2B). Endogenous KHC was efficiently precipitated by an anti-KHC antibody (Figure 2B), along with mNUDC, DIC and $P150^{Glued}$, but these proteins were not precipitated with the control serum. We further examined immunoprecipitation by an anti-DIC antibody, and found co-precipitation of KHC with DIC (Figure 2C), consistent with direct binding of DIC to KLC1 or KLC2 by yeast two-hybrid and affinity chromatography, as previously reported (Ligon *et al*, 2004). We therefore addressed whether mNUDC is required for interaction of cytoplasmic dynein with kinesin-1 by an immunoabsorption assay. An anti-mNUDC antibody efficiently removed endogenous mNUDC from the DRG extract (Figure 2D), resulting in a suppression of immunoprecipitation of DIC and $P150^{Glued}$ with KHC or immunoprecipitation of KHC with DIC (Figure 2E and F), suggesting that binding of DIC and KHC was mediated by mNUDC. Much of axonal transport is vesicular. We therefore examined whether the anterograde transport of dynein was mediated by a protein complex or within the context of a vesicle. To address this issue, we performed immunoprecipitation without or with detergent (0.3% NP-40) to disrupt vesicles. Immunoprecipitation of DIC and $P150^{Glued}$ with KHC or immunoprecipitation of KHC with DIC was similar in the presence or absence of detergent (Figure 2G and H), suggesting the presence of vesicle-independent protein complexes. We examined direct protein interactions by pull-down assays using recombinant proteins expressed in bacteria. We were not able to find direct interaction of mNUDC with KHC (data not shown), whereas clear interaction of mNUDC and KLC1 was detected (Figure 2I and J). We also performed MT pull-down assay under presence or absence of mNUDC (Figure 2K and L). Although the precipitation of kinesin-1 with MTs was mildly augmented by the presence of mNUDC, this augmentation was not significant.

Knockdown of mNUDC by siRNA results in abnormal localization of dynein components and membranous organelles

To determine the role of mNUDC in the regulation of cytoplasmic dynein and dynactins, we downregulated endogenous mNUDC by RNAi and examined the effects of *mNudC* gene silencing on mNUDC levels and distribution of LIS1, NDEL1, cytoplasmic dynein and dynactins. Cells transfected with mNUDC siRNA displayed a reproducible and significant

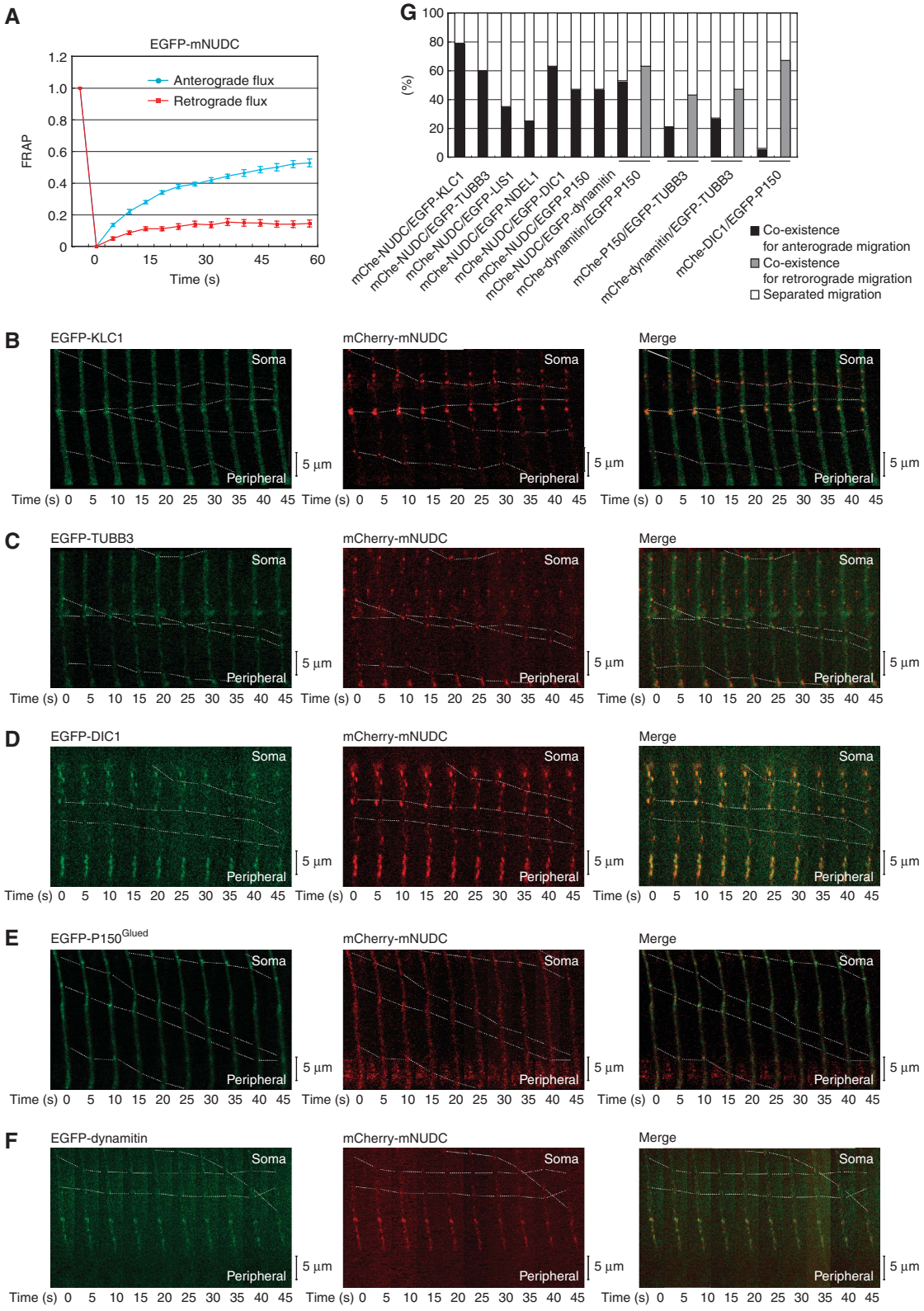

Figure 1 Dynamics of mNUDC in dorsal root ganglia (DRG) neuron. FRAP analysis of DRG neuron expressing EGFP–mNUDC proteins. The graph shows the relative fluorescent recovery directly after bleaching. The pre-bleach level is normalized to 1. (**A**) EGFP–mNUDC recovery. (**B**) EGFP–KLC1, (**C**) EGFP–TUBB3 (tubulin β3), (**D**) EGFP–DIC1, (**E**) EGFP–P150^{Glued}, (**F**) EGFP–dynamitin with mCherry–mNUDC. Note: dotted lines indicate corresponding particles. Downward movement indicates anterograde transport by kinesin-1. (**G**) Co-migration frequency of fluorescence-tagged proteins in DRG neurons. Black portion (anterograde transport) or grey portion (retrograde transport) indicates the frequency of co-migration, whereas the rest of the white portion indicates the frequency of separated migration. Combinations of fluorescence-tagged proteins are indicated at the bottom.

(>80%) reduction in the amount of steady-state 42-kDa mNUDC protein 48 h after transfection (Figure 3A, left panel). By contrast, mNUDC levels in cells transfected with control siRNA were unaffected (Figure 3A, right panel). We co-transfected a control GFP vector to monitor cell shape and avoid misinterpretation of our results due to alteration of cell shape. In control cells, cytoplasmic dynein, LIS1, NDEL1, $P150^{Glued}$ and dynamitin exhibited a dispersed outward distribution with a gradient emanating from the centrosome, whereas mNUDC-depleted cells displayed an abnormal perinuclear accumulation (Figure 3B and D). We further examined the effect of depletion of mNUDC on the distribution of membranous organelles. In control cells, mitochondria, lysosomes, β-COP-positive vesicles and early endosomes were distributed homogenously within the cell. In sharp contrast, mNUDC-depleted cells displayed abnormal perinuc-

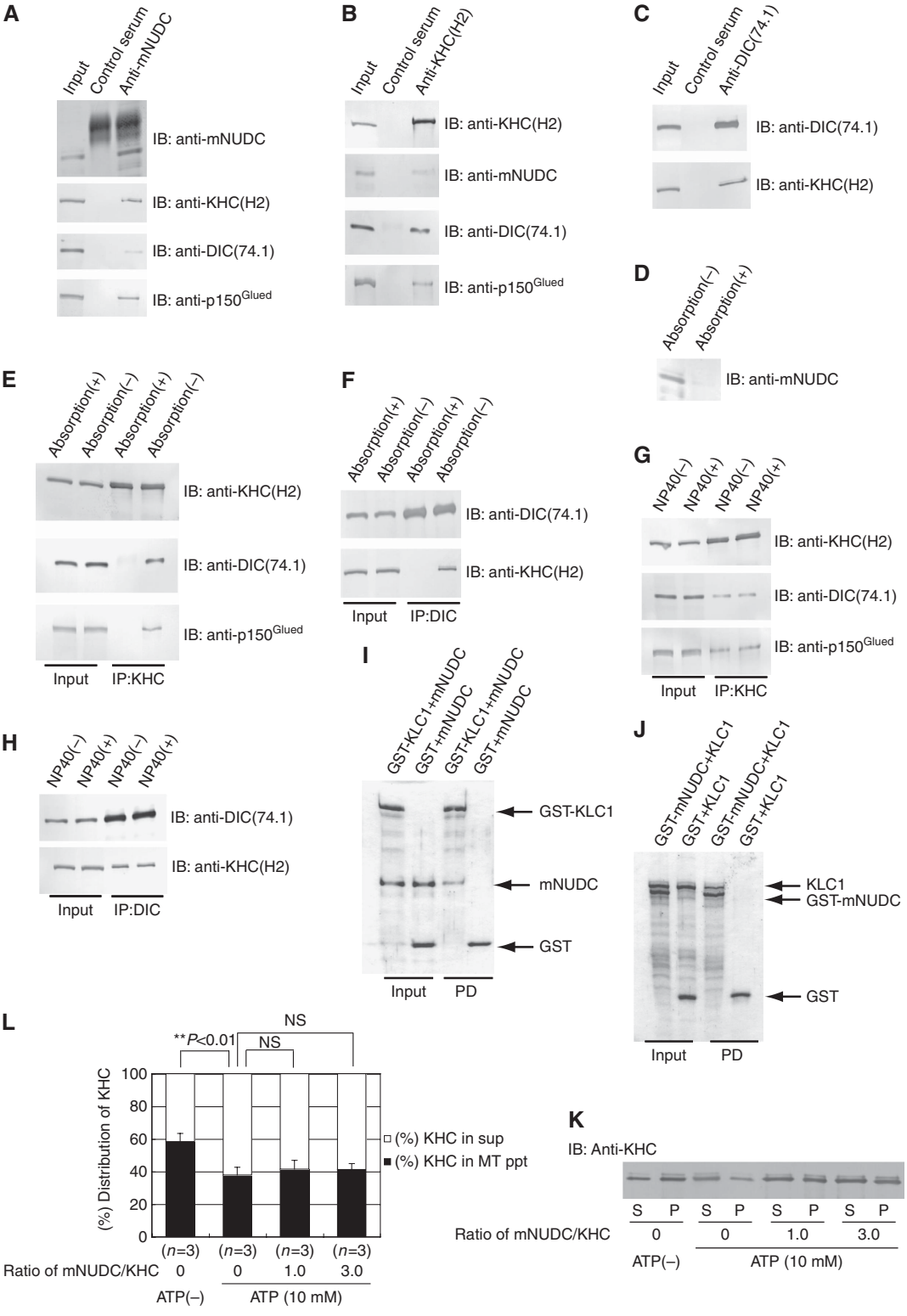

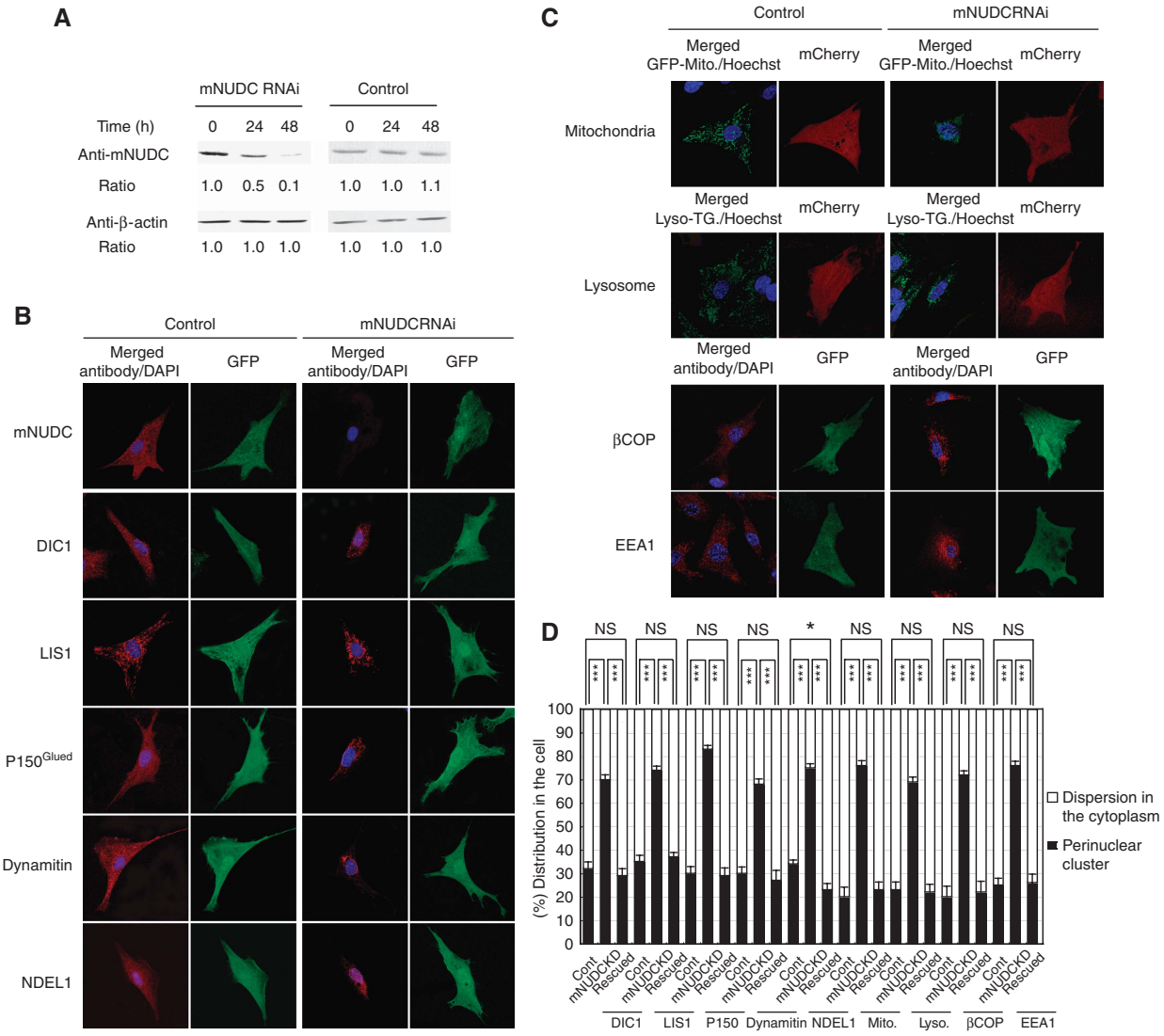

Figure 3 Depletion of mNUDC by siRNA displays severe perturbation of cytoplasmic dynein and dynactins. (**A**) Downregulation of mNUDC by siRNA. Extracts from mouse embryonic fibroblast (MEF) cells transfected with siRNA–mNUDC or control siRNA collected at different time points were immunoblotted with an anti-mNUDC antibody and an anti-βactin. (**B**) Depletion of mNUDC induces perinuclear accumulation of dynein intermediate chain1 (DIC1), LIS1, P150^{Glued}, dynamitin and NDEL1. (**C**) Depletion of mNUDC induces aberrant distributions of membranous organelles, including mitochondria, lysosomes, β-COP and endosomes. (**D**) Statistical analysis of each distribution in MEF cells. Compared with control, mNUDC was depleted by siRNA and rescued by mutated CFP–mNUDC. The *P*-value was calculated using Student's *t*-test.

Figure 2 mNUDC is required for the formation of complexes of kinesin with P150^{Glued} and DIC. Total cell extracts from mouse brain were subjected to immunoprecipitation with (**A**) an anti-mNUDC antibody, (**B**) an anti-KHC(H2) antibody and (**C**) an anti-DIC(74.1) antibody. About 5% of the input (pre-IP) and 20% the immunoprecipitates (post-IP) were separated by SDS–PAGE and western blot with antibodies against the proteins are indicated on the right side. One of three independent experiments is shown. (**D**) Endogenous mNUDC was immunoabsorbed from brain extract. Immunoabsorption clearly removed endogenous mNUDC. mNUDC removed brain extracts were immunoprecipitated (**E**) with an anti-KHC(H2) antibody and (**F**) with an anti-DIC(74.1) antibody. About 5% of the input (pre-IP) and 20% the immunoprecipitates (post-IP) were separated by SDS–PAGE and western blot with antibodies against the proteins are indicated on the right side. One of three independent experiments is shown. Note: Co-precipitates of KHC, P150^{Glued} and DIC disappeared after immunoabsorption by an anti-mNUDC antibody. Total cell extracts from mouse brain were subjected to immunoprecipitation (**G**) with an anti-KHC(H2) antibody and (**H**) with an anti-DIC(74.1) antibody under presence (0.3% NP-40) or absence of detergent. About 5% of the input (pre-IP) and 20% the immunoprecipitates (post-IP) were separated by SDS–PAGE and western blot with antibodies against the proteins are indicated on the right side. One of three independent experiments is shown. Note: detergent did not affect co-immunoprecipitation, suggesting that the binding of KHC and DIC was not mediated by membranous structures. Pull-down assays using recombinant protein expressed in bacteria. (**I**) Pull-down by GST–KLC1 or (**J**) GST–mNUDC. Untagged mNUDC and untagged KLC1 were precipitated with GST–KLC1 and GST–mNUDC, respectively. GST was used as negative control. About 20% of the input and the pull-down precipitates were separated by SDS–PAGE and stained by Comassie brilliant blue. (**K**, **L**) Microtubule pull-down assay. We examined whether mNUDC augments precipitation of kinesin-1 with microtubules. In comparison with absence of ATP condition, presence of ATP facilitated dissociation of kinesin-1 from microtubules, indicating that kinesin-1 is functionally active (**$P<0.01$). Under the presence of ATP, mNUDC slightly augmented precipitation of kinesin-1 with microtubules, but it was not statistically significant (NS: not significant). We performed three independent sets of experiments. S and P indicate supernatant and precipitant, respectively.

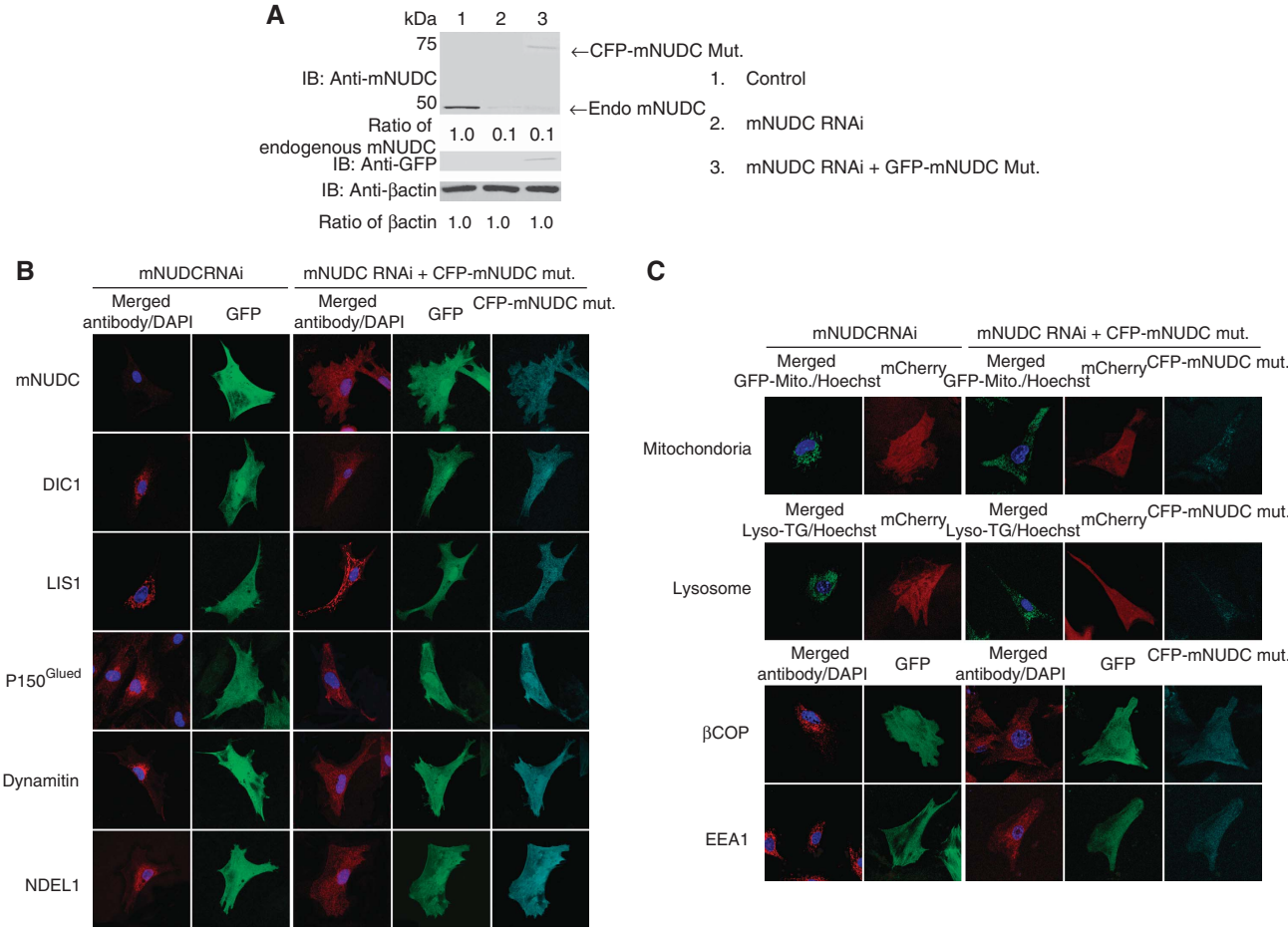

Figure 4 Rescue experiments of depletion of mNUDC by siRNA by the expression of mutated mNUDC. (**A**) We introduced mutations overlapping the siRNA region, which do not change the amino-acid sequence. (**B**) The expression of mutated *CFP–mNudC* construct clearly rescued aberrant distribution of DIC1, LIS1, P150^{Glued}, dynamitin and NDEL1. (**C**) Aberrant distributions of membranous organelles, including mitochondria, lysosomes, β-COP and endosomes by depletion of mNUDC were also rescued by the expression of mutated *CFP–mNudC*.

lear clustering (Figure 3C and D). These mislocalizations were clearly rescued by exogenous expression of siRNA-resistant CFP–mNUDC (Figures 3D and 4), suggesting that mNUDC may be required for anterograde transport of these components.

mNUDC is required for anterograde transport of cytoplasmic dynein and a dynactin complex

We next wanted to know whether mNUDC is required for anterograde transport of cytoplasmic dynein and dynactins. Functional analysis of mNUDC by siRNA-mediated depletion was technically challenging, as the slow loss of mNUDC resulted in death of the DRGs, similar to the effect of loss of LIS1. We therefore analysed the anterograde dynamics of each protein by treatment of DRG neurons with blocking antibodies against mNUDC (Yamada *et al*, 2008) (Supplementary Figure S2A). The administration of an anti-mNUDC antibody for 1 min to permeabilized DRG neurons clearly abolished anterograde transport of mNUDC, suggesting that this antibody effectively blocked mNUDC function (Supplementary Figure S3C). Although mNUDC antibody treatment did not affect the anterograde movement of kinesin-1 (Figure 5A), anterograde transport of TUBB3 and DIC1 was severely perturbed in the presence of this antibody (Figure 5B and C). These findings suggest that mNUDC connects kinesin-1 and a tMT–LIS1–cytoplasmic dynein complex (see Figure 8).

We next addressed whether mNUDC is involved in the transport of P150^{Glued} and dynamitin. Blocking of mNUDC function by the inhibitory antibody completely suppressed anterograde transport of GFP–P150^{Glued} and GFP–dynamitin (Figure 5D and E), suggesting that mNUDC also functions to connect kinesin-1 and dynactins. We inversely examined whether blocking antibodies against P150^{Glued} or dynamitin interfere with anterograde transport of other molecules. We first confirmed that blocking antibodies against P150^{Glued} and dynamitin efficiently abolished anterograde and retrograde movements of P150^{Glued} and dynamitin, respectively (Supplementary Figure S3D and E). Suppression of P150^{Glued} or dynamitin by these blocking antibodies failed to display any suppressive effect on the anterograde transport of mNUDC (Supplementary Figure S3F and G), suggesting that P150^{Glued} or dynamitin are not required for the binding of mNUDC with kinesin-1.

A cytoplasmic dynein complex and a dynactin complex are separately transported to the plus-end of MTs

A tMT–LIS1–cytoplasmic dynein complex, as well as P150^{Glued} and dynamitin are transported to the plus-end of MTs in an mNUDC-dependent manner, although it was unclear whether they were all transported as a single complex.

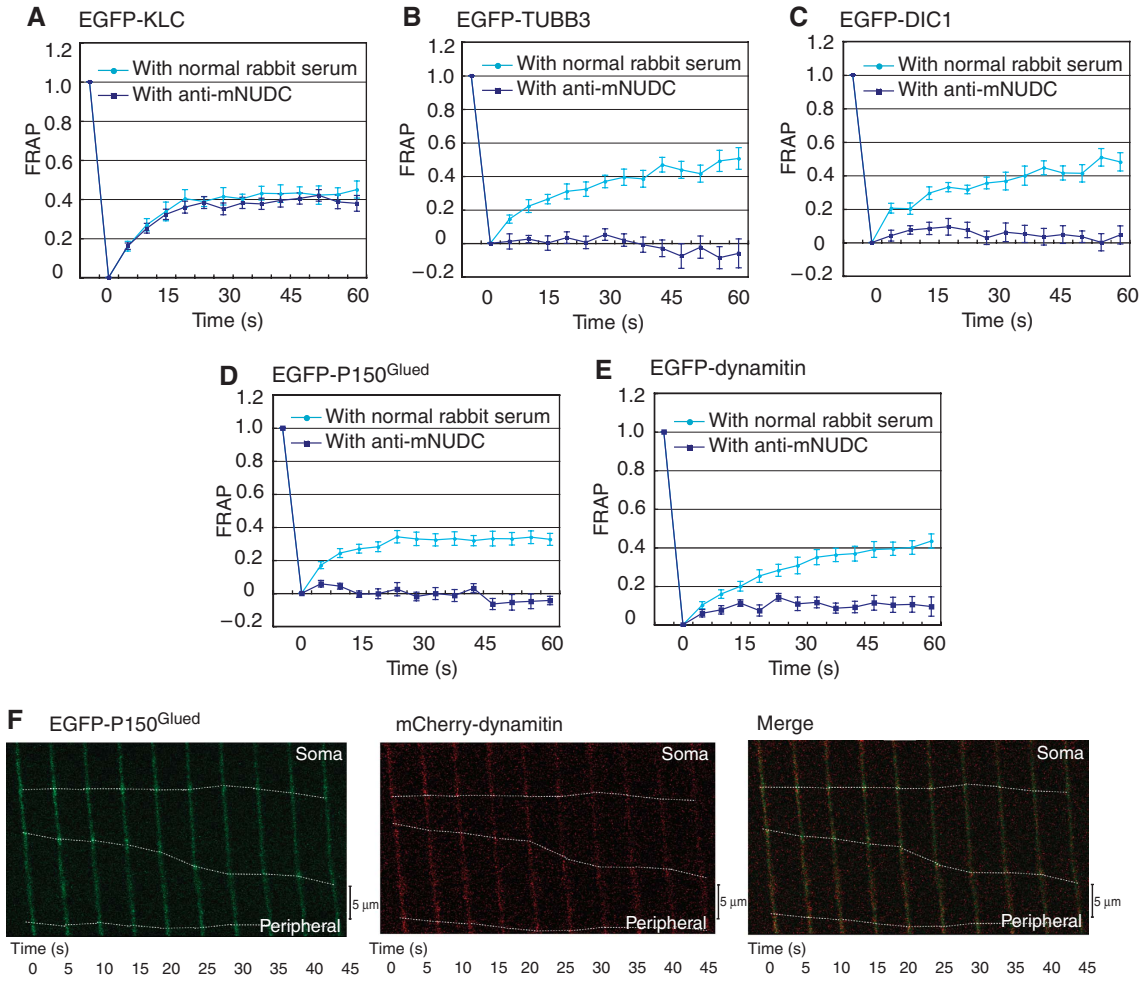

Figure 5 FRAP analysis of dynamics of cytoplasmic dynein and dynactins in the presence of an anti-mNUDC antibody. FRAP analysis of DRG neurons expressing: (**A**) EGFP–KLC1, (**B**) EGFP–TUBB3, (**C**) EGFP–DIC1, (**D**) EGFP–P150^{Glued}, (**E**) EGFP–dynamitin with an anti-mNUDC antibody. DRG neurons were permeabilized followed by 1-min incubation of a blocking antibody before observation. Although anterograde movement of KLC was intact, anterograde transport of DIC1, TUBB3, P150^{Glued} and dynamitin were completely suppressed by inhibition of mNUDC. (**F**) Imaging of dynamic co-localization of EGFP–P150^{Glued} and mCherry–dynamitin in DRG neurons. Note: EGFP–P150^{Glued} and mCherry–dynamitin are co-migrating during anterograde transport. Downward movement indicates the anterograde transport by kinesin-1.

Before addressing this issue, we first examined the co-migration of P150^{Glued} and dynamitin during anterograde transport. P150^{Glued} and dynamitin frequently co-migrated (Figures 1G and 5F: P150^{Glued}/dynamitin (anterograde), 53%), and the frequency of co-migration was similar during anterograde and retrograde movement (Figure 1G: P150^{Glued}/dynamitin (anterograde), 53%; P150^{Glued}/dynamitin (retrograde), 63%), suggesting that P150^{Glued} and dynamitin are part of the same complex during anterograde transport. Inhibition of P150^{Glued} by a blocking antibody did not exhibit any suppressive effect on anterograde transport of KLC1, TUBB3 and DIC1 (Figure 6A–C), and similar results were found after functionally blocking dynamitin (data not shown), suggesting that dynactins are not essential components for anterograde transport of a tMT–LIS1–cytoplasmic dynein complex. We further explored co-migration of DIC1 and P150^{Glued}, and found less frequent co-migration of these two proteins than the co-migration of either protein with mNUDC (Figures 1G and 6D: DIC1/P150^{Glued}, 6%), whereas DIC1 and P150^{Glued} co-migrated frequently in retrograde transport (Figure 1G and 6D: DIC1/P150^{Glued}, 67%). These data suggest that dynactins are not co-migrating with a cytoplasmic dynein complex. Instead, cytoplasmic dynein and dynactin are separately transported to the plus-end of MTs.

We next examined whether blocking of either P150^{Glued} or dynamitin perturb transport of other components. Suppression of P150^{Glued} and dynamitin by a blocking antibody completely abolished retrograde transport of P150^{Glued}, dynamitin and DIC1 (Figure 6E–G). In clear contrast, blocking of P150^{Glued} did not perturb anterograde transport of dynamitin (Figure 6F and Table I), and other components (data not shown). Interestingly, although blocking of dynamitin did not perturb the anterograde transport of DIC (data not shown), it did suppress anterograde transport of P150^{Glued} (Figure 6E and Table I). These results imply that dynamitin is required for stable binding of P150^{Glued} to other dynactin components, including Arp1, whereas P150^{Glued} is not required for binding of dynamitin to Arp1, which is consistent with previous reports (Echeverri *et al*, 1996; Eckley *et al*, 1999). However, removal of dynamitin did not suppress binding of P150^{Glued} to other dynactin components, which might imply that P150^{Glued} is capable of binding to Arp1 directly, and that dynamitin is required for making a more stable complex.

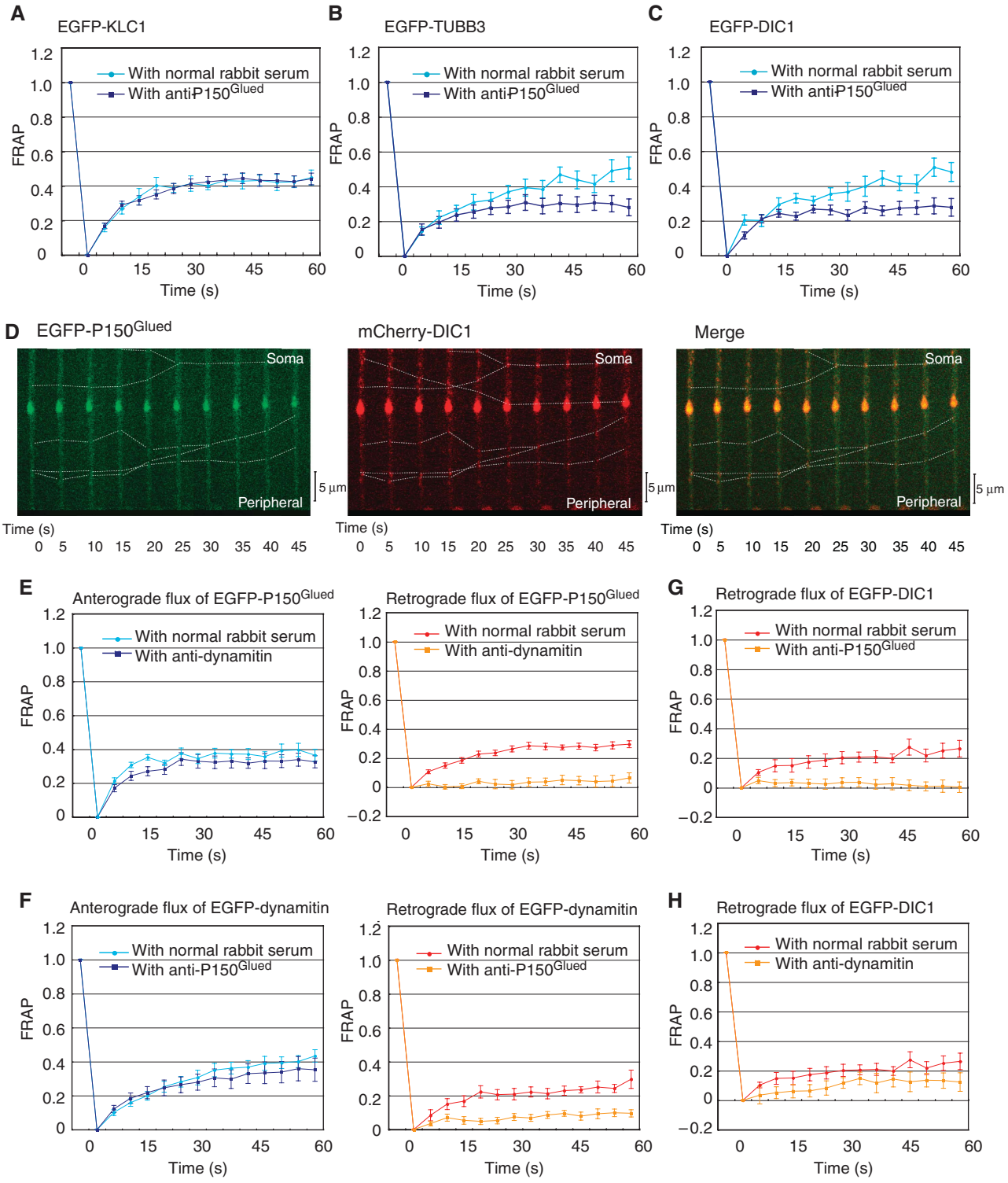

Figure 6 Separate movement of a cytoplasmic dynein complex and a dynactin complex. FRAP analysis of DRG neurons expressing (**A**) EGFP–KLC1, (**B**) EGFP–TUBB3 and (**C**) EGFP–DIC1 with an anti-P150^{Glued} antibody. Note: inhibition of P150^{Glued} did not affect anterograde transport of kinesin-1, TUBB3 or DIC1. (**D**) Imaging of co-migration of EGFP–DIC1 and mCherry–P150^{Glued} in DRG neurons. Note: P150^{Glued} clearly co-migrated with DIC1 in retrograde transport, whereas they displayed distinct, non-overlapping behaviour in anterograde movement, suggesting that they are separately transported during anterograde movement. Downward movement indicates the anterograde transport by kinesin-1, whereas upward movement indicates the retrograde transport by cytoplasmic dynein. FRAP analysis of DRG neurons expressing (**E**) EGFP–P150^{Glued} with an anti-dynamitin antibody, (**F**) EGFP–dynamitin with an anti-P150^{Glued} antibody, (**G**) EGFP–DIC1 with an anti-P150^{Glued} antibody and (**H**) EGFP–DIC1 with an anti-dynamitin antibody. DRG neurons were permeabilized followed by 1-min incubation of a blocking antibody before observation. Note: the presence of antibodies severely perturbed the recovery by retrograde movement, whereas anterograde movement was fairly intact.

Table I Changes in $t_{1/2}$ (s) of fluorescence recovery with anti-dynamitin or anti $P150^{Glued}$ antibody

EGFs	Antibody	$t_{1/2} \pm$ s.e.m. (s)	
EGFP–P150	Normal rabbit serum	4.3 ± 0.62	]**
	Anti-dynamitin	7.1 ± 0.58	
EGFP–dynamitin	Normal rabbit serum	11.9 ± 1.02	]NS
	Anti-P150	10.8 ± 1.62	

NS, not significant.
The fluorescence recoveries of EGFP–dynamitin were not significantly changed with anti- $P150^{Glued}$ antibody, whereas the recoveries of EGFP–$P150^{Glued}$ displayed significant reduction with anti-dynamitin antibody. $^{**}P<0.01$.

Recombinant mNUDC supports the transport of MTs and dynactin by purified kinesin-1

Our data suggest that mNUDC mediates binding of tMT–LIS1–cytoplasmic dynein complex and dynactins with kinesin-1 for anterograde transport. To obtain more conclusive direct evidence, we performed *in vitro* transport experiments using recombinant mNUDC and native kinesin-1 purified from porcine brain. Taxol-stabilized fluorescence-labelled (FL-Cy3, -Cy5 or -tetramethyl rhodamine (TMRA)) MTs were adsorbed onto the surface of a microscope perfusion chamber, fixed as 'rails.' Next, pre-incubated mixtures of native kinesin-1, FL-labelled soluble MTs ('transportable MTs'), and FL-labelled dynactin components and recombinant mNUDC were introduced. Interestingly, a substantial fraction of native kinesin-1 purified from porcine brain also contained endogenous mNUDC (Figure 7A). Quantitative western blotting using recombinant or purified protein as references revealed that the molecular ratio of endogenous mNUDC and kinesin-1 is 1.00:2.89 (Figure 7B and C). To examine the effect of mNUDC in this *in vitro* reconstruction assay, we removed endogenous mNUDC by immunoabsorption using an anti-mNUDC antibody to obtain mNUDC-free kinesin-1 (Figure 7A). The purified kinesin fraction displayed MT-activated ATPase activity regardless of whether endogenous mNUDC was bound or not (data not shown). This ATPase activity was not influenced by the addition of recombinant mNUDC, suggesting that mNUDC is not essential for ATP hydrolysis. We optimized the conditions for *in vitro* transport experiments to avoid any confusion derived from transport by kinesin-1 that was attached to the chamber surface directly. In the absence of attached rail MTs, FL-labelled transportable MTs were rarely attached on the surface of a perfusion chamber (Figure 7D, column 1). Furthermore, no obvious movement of FL-labelled transportable MTs was detected. We next wanted to exclude the possibility of non-specific binding of FL-labelled transportable MTs on the surface of a perfusion chamber. We examined the frequency of FL-labelled transportable MTs in the presence of FL-labelled rail MTs without kinesin-1, and found no attachment of FL-labelled transportable MTs (Figure 7D, column 2), indicating that non-specific binding of FL-labelled transportable MTs was extremely low. In addition, we also confirmed that recombinant mNUDC does not tether MTs, and thereby does not confer artificial activation when MTs are in close proximity (Figure 7D, column 4). Thus, we concluded that attachment of FL-labelled transportable MTs was mediated by kinesin-1 that bound rail MTs on the surface of a perfusion chamber, and its movement was driven by kinesin-1. We examined the effect of mNUDC-free kinesin-1, and found no obvious attachment and transport of FL-labelled transportable MTs (Figure 7D, column 3), suggesting that mNUDC-free kinesin-1 is incapable of binding and transporting MTs. In sharp contrast, addition of recombinant mNUDC dramatically facilitated the attachment of FL-labelled transportable MTs (Figure 7D, column 5; Supplementary Movie 6). In addition, the transport of 62.5% of attached FL-labelled transportable MTs was seen (Figure 7D, column 5). The velocity of transport for mNUDC and kinesin-1-mediated MTs was 0.47 ± 0.07 μm/s, which is similar to the rates of regular speed of kinesin-1 (Vale *et al*, 1985a, b). We next examined the effect of native kinesin-1 that was not depleted of endogenous mNUDC. Interestingly, native kinesin-1 transported FL-labelled transportable MTs efficiently (Figure 7D, column 6, 23.9%), suggesting that a substantial fraction of native kinein-1 contains endogenous mNUDC. We further examined the behaviour of FL-labelled transportable MTs in the presence of mNUDC-depleted kinesin-1, recombinant mNUDC and a blocking antibody against mNUDC. In this case, the effect of the addition of recombinant mNUDC was completely erased by a blocking antibody against mNUDC, and FL-labelled transportable MTs were unable to attach (Figure 7D, column 7). Finally, we examined whether the *in vitro* motility assay is inhibited by AMPPNP (Figure 7D, column 8) or EHNA (Figure 7D, column 9) as a control. AMPPNP clearly inhibited motile MTs, whereas EHNA displayed only a mild suppressive effect (21.9%). These observations demonstrated that mNUDC is essential for binding of MTs with kinesin-1 to transport MTs. We further examined whether mNUDC directly binds MTs through an MT pull-down assay (Supplementary Figure S4A and B). In the absence of MTs, mNUDC were detectably precipitated (lane 1, 2). In contrast, mNUDC precipitation was clearly increased in the presence of MTs (lane 5, 6), an increase that was slightly augmented by addition of kinesin-1 (lane 9, 10), suggesting that mNUDC directly binds to MTs (see Discussion section).

We next addressed whether mNUDC is able to mediate the attachment and transport of dynactins and kinesin-1. We purified a dynactin complex from porcine brains, and obtained highly purified dynactins (Figure 7E). In this case, we used native kinesin-1 in which endogenous mNUDC was not depleted. We optimized conditions such that FL-labelled dynactins were rarely attached on the surface of a perfusion chamber in the absence of FL-labelled 'rail' MTs attached to the surface (Figure 7F, column 1). Without native kinesin-1, only a small fraction of dynactin was attached, and mobile FL-labelled dynactins were not observed (Figure 7F, column 2), suggesting that the observed movement was due to moving dynactin particles instead of artificial dynactin particles that are stuck to moving MTs. We also confirmed that recombinant mNUDC does not tether MTs and dynactins, and therefore does not result in artificial activation when MTs and dynactins are in close proximity (Figure 7F, column 4). We next added native kinesin-1 and found only marginal facilitation of the attachment of FL-labelled dynactins that remained immobile (Figure 7F, column 3). Further addition of recombinant mNUDC to native kinesin-1 resulted in the significant augmentation of attached FL-labelled dynactins (Figure 7F, column 5; Supplementary Movie 7). Although it was not as efficient as with MTs, additional recombinant

mNUDC clearly stimulated movement of FL-labelled dynactins (Figure 7F, column 5, 18.5%). These effects of recombinant mNUDC were completely abolished by the addition of a blocking antibody against mNUDC (Figure 7F, column 6). Finally, we examined whether this motility of dynactin was inhibited by AMPPNP (Figure 7F, column 7) or EHNA (Figure 7F, column 8) as a control. AMPPNP clearly inhibited motile dynactins, whereas EHNA displayed only a mild suppressive effect (15.6%). These results indicate that the mNUDC is sufficient for mediating attachment of dynactins and transport in this *in vitro* assay. A dynactin complex is capable of binding MTs directly, and thereby might be

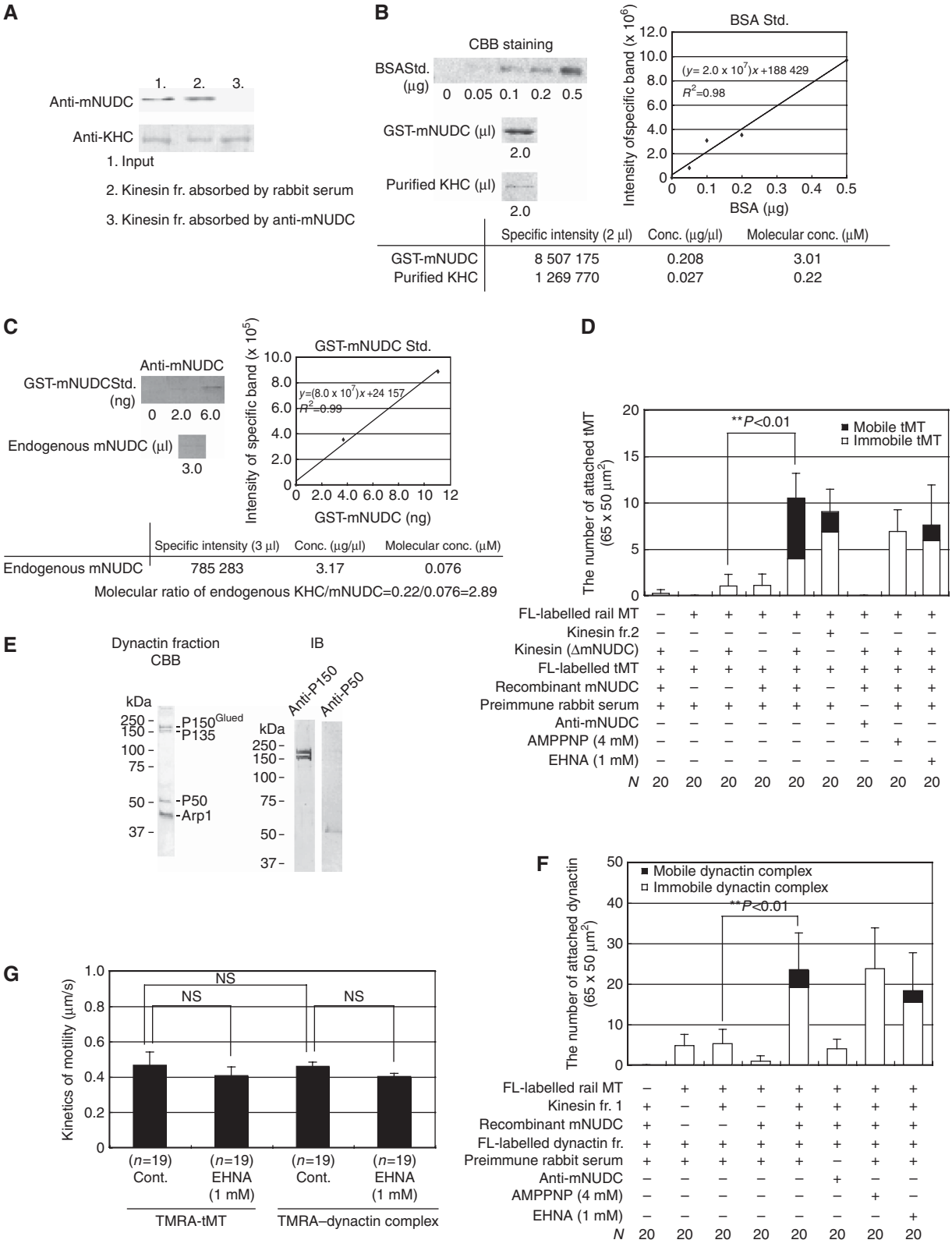

transported as a complex with MTs. Further experiments will be need to provide supporting evidence for this possibility. Although EHNA displayed a mild suppressive effect on the motility of MTs or dynactins, EHNA did not perturb the speed of kinesin-1-dependent transport of both components (Figure 7G).

Discussion

Here, we report that mNUDC is an essential protein that connects kinesin-1 with a cytoplasmic dynein complex and an apparently distinct dynactin complex. Inhibition of mNUDC resulted in severe perturbation of anterograde transport, including a cytoplasmic dynein–LIS1–tMT complex, and a dynactin complex (Figure 8). Inhibition of mNUDC abolished anterograde transport of membranous organelles, including mitochondria and lysosomes. The siRNA-mediated depletion of mNUDC also perturbed subcellular distributions of these organelles, suggesting that mNUDC might be a broadly acting adaptor molecule for kinesin-1. By contrast, motility of KLC1 was maintained nearly intact after depletion of mNUDC (Gindhart *et al*, 1998; Rahman *et al*, 1999), supporting the interpretation that mNUDC is an adaptor rather than a functional component of kinesin-1-like kinesin light chains. Our *in vitro* transport assay also shows that mNUDC is required for MT binding and transport by kinesin-1. Kinesin-1 transported a substantial fraction of MTs after the addition of recombinant mNUDC (62.5%), whereas recombinant mNUDC moderately facilitated the attachment and movement of dynactins (18.5%).

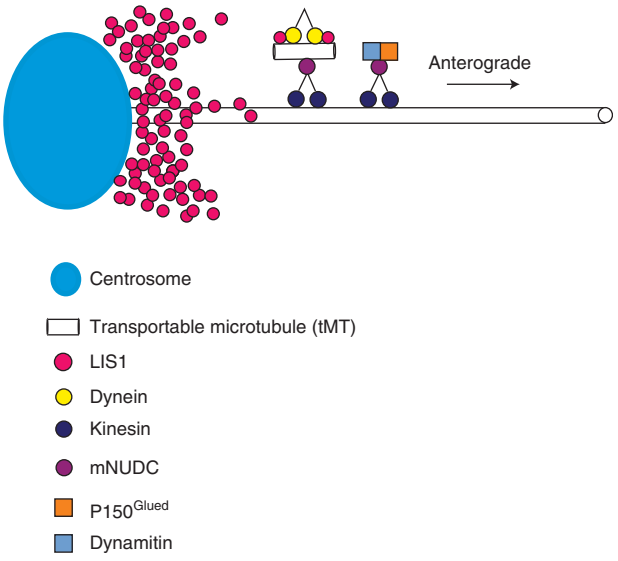

Figure 8 Model for the regulation of protein and organelle transport by mNUDC. Schematic representation of the role of mNUDC as an adaptor molecule for anterograde transport by kinesin-1. mNUDC mediates the connection between MTs and dynactins.

Although these findings provide important insights into the transport of dyneins and dynactins by kinesin via mNUDC, the complete elucidation of a mechanism by which a dynein complex or a dynactin complex is transported by kinesin-1 will require further studies. First, the precise structure of MTs used for transport of cytoplasmic dynein is not known, nor is it known whether there is a clear distinction between transportable and stationary MTs *in vivo*. mNUDC might bind microtubules through accessory microtubule-associated proteins that were co-purified with tubulin, instead of directly binding to microtubules. Second, the reason for less efficient facilitation of dynactin transport remains unknown. For *in vivo* transport of dynactins, it is possible that additional components are required to mediate binding of dynactins and kinesin-1. It is known that the ATPase cycle of kinesins-1 is allosterically controlled by microtubule binding (Kuznetsov and Gelfand, 1986), and kinesin-1 switches from an inhibited state to a motile state upon cargo binding (Hackney *et al*, 1992; Stock *et al*, 1999). To address precise structures of kinesin-1-dependent transport, characterization of each kinesin–cargo complex is required. Third, much of axonal transport is vesicular. Our experiments suggest that anterograde transport of dynein or dynactins is vesicle independent. Further characterization of kinesin–cargo complex is required to address these remaining questions.

The activation of cytoplasmic dynein requires dynactins, a complex that contains multiple subunits, including the 150-kDa dynactin protein and the actin-related proteins: Arp1 and Arp11 (Holleran *et al*, 1998). Our previous study discovered that cytoplasmic dynein moves in an outward direction

Figure 7 *In vitro* transport experiments using purified native kinesin from porcine brains and recombinant mNUDC. (**A**) Immunoabsorption of endogenous mNUDC by an anti-mNUDC antibody. We found a substantial amount of purified kinesin-1 was bound by endogenous mNUDC (lane 1). We removed this endogenous, bound mNUDC in the observation chamber by immunoabsorption using an anti-mNUDC antibody, which efficiently removed endogenous mNUDC (lane 3). (**B**) Quantitative western blotting for endogenous mNUDC bound to kinesin-1. For determination of molecular ratio between kinesin-1 and mNUDC, we first made a calibration curve on the basis of the intensity of CBB staining using BSA as reference. The summary is shown at the bottom. In these experiments, we define the concentration of recombinant mNUDC (0.208 μg/μl, 3.01 μM) and purified kinesin-1 (0.027 μg/μl, 0.22 μM). (**C**) Using the above information, we determined the concentration of mNUDC bound to kinesin-1 by western blotting. Recombinant mNUDC used for reference disclosed the concentration of mNUDC bound to kinesin-1 (3.17 μg/μl, 0.076 μM). Finally, we calculated the ratio of kinesin-1:mNUDC as 2.89. (**D**) Examination of FL-labelled transportable MTs behaviour. Open column indicates immobile attachment of FL-labelled transportable MTs on the observation chamber, whereas solid column indicates mobile FL-labelled transportable MTs. Combinations of introduced proteins are shown on the left. The total numbers of observed chambers are shown on the bottom. Note: addition of recombinant mNUDC dramatically facilitated the attachment of FL-labelled transportable MTs, and stimulated their transport by kinesin-1 (column 5). Interestingly, native kinesin in which endogenous mNUDC was not removed displayed similar pattern with kinesin-1 supplemented with recombinant mNUDC (column 6). (**E**) Comassie brilliant blue staining and western blotting analysis of purified dynactins. The dyanctin fraction was highly purified, and contaminated proteins were not detectable. (**F**) Examination of FL-labelled dynactin behaviour. Open column indicates immobile attachment of FL-labelled dynactins on the observation chamber, whereas solid column indicates mobile FL-labelled dynactins. Combinations of introduced proteins are shown on the left. Total numbers of observed chambers are shown on the bottom. Note: additional recombinant mNUDC dramatically facilitated attachment of FL-labelled dynactins. Additional recombinant mNUDC stimulated their transport by kinesin-1, but it was less efficient than MTs (column 5). (**G**) Comparison of transport speed of MTs or dynactins by kinesin-1 between under the presence and the absence of EHNA conditions. The *P*-value was calculated using Student's *t*-test. NS indicates not significant.

towards the plus ends on the transportable MTs as cytoplasmic dynein is held in an inactive form (Yamada *et al*, 2008), However, the underlying mechanism by which cytoplasmic dynein is insulated from its activating machinery was unknown. Our studies provide a potential mechanism for this observation. We unexpectedly discovered that a dynactin complex is transported in a separate mNUDC–kinesin-1 complex to the plus-end of MTs distinct from the tMT–LIS1–cytoplasmic dynein complex. Dynactin enhances the processivity of the dynein motor and also mediates some interactions with cargoes, which is essential for retrograde transport (Schroer, 2004). In fact, inhibition of either $P150^{Glued}$ or dynamitin by blocking antibodies severely perturbed retrograde transport of cytoplasmic dynein. Presumably, the independent transport of these two components ensures that the retrograde transport activity of cytoplasmic dynein is inactive during anterograde transport of dynein to the plus-end, and these two components may be assembled thereafter to activate dynein as a retrograde motor.

Our model for a mechanism by which cytoplasmic dynein is transported to the plus-end of MTs will provide an explanation for the puzzling observations made by several investigators that the normal broad cytoplasmic distribution of components of the LIS1–NDEL1–cytoplasmic dynein complex are localized in a perinuclear pattern when any of these components, especially LIS1, is reduced (Niethammer *et al*, 2000; Sasaki *et al*, 2000; Smith *et al*, 2000; Toyo-oka *et al*, 2003; Yingling *et al*, 2008). It also provides an explanation for the observation that loss of LIS1 results in reduction of astral mictrotubules, reduction of cortical dynein and impairment of cortical microtubule capture in mitotic cells (Faulkner *et al*, 2000; Yingling *et al*, 2008). mNUDC is essential for the binding of kinesin-1 and the cytoplasmic dynein–LIS1–tMT complex, and reduction of mNUDC results in mitotic defects (Aumais *et al*, 2003). It is likely that some of the mitotic defects displayed by LIS1-deficient cells result from disruption of the kinesin-mediated transport of dynein as seen after depletion of mNUDC. However, mitotic cells lack the long processes of neuronal cells, and also have a high soluble pool of dynein. Recruitment from this soluble pool in spherical cells with a much smaller diameter may be sufficient to support mitosis, and there may be little contribution of LIS1-mediated transport of dynein to the overall dynein supply in such cells. Context-specific mechanisms of dynein transport are further questions that will be addressed in future experiments.

Nuclear migration has a fundamental developmental role in many higher and lower eukaryotes. Genetic analysis of nuclear migration in *A. nidulans* has led to the identification of a large number of proteins involved in this process and are referred to as nud genes (Morris *et al*, 1998a). These nud genes are classified into three categories, that is, *nudA* and *nudG* encode cytoplasmic dynein heavy chain and light chain, respectively (Morris *et al*, 1998a, 1998b). These genes are motor proteins and its accessory molecules. However, *nudK* and *nudM* encode actin-related proteins and $P150^{Glued}$, respectively, which are part of dynactin (Xiang *et al*, 1999; Zhang *et al*, 2003). *Nde1/Ndel1* and *Lis1* are mammalian homologues of *nudE* and *nudF*, which are required for the regulation and localization of cytoplasmic dynein (Xiang *et al*, 1995). Our findings uncovered the new role of mNUDC as an adaptor molecule of kinesin-1. Thus, mNUDC could be considered as a gene in a new fourth category, which includes proteins that mediate interactions between kinesin-1 and cytoplasmic dynein. Interestingly, there are other mNUDC family proteins in mammals. For example, depletion of mammalian NudC-like protein (NudCL) by RNAi in HeLa cells inhibits cell growth and induces mitotic arrest with multiple mitotic defects, which subsequently result in cell death (Zhou *et al*, 2006). In addition, depletion of NudCL also results in the aggregation of dynein intermediate chain throughout the cytoplasm during mitosis (Zhou *et al*, 2006). Although the precise characterization of this family of proteins has not yet been performed, it is possible that they may have a broad range of functions to facilitate binding of kinesin-1 to target molecules or organelles. This new role for mNUDC will be useful for the understanding of the crosstalk between cytoplasmic dynein and kinesin-1.

Materials and methods

Vectors used for expression in DRG and recombinant proteins

The complementary DNAs carrying full length of open reading frame of each of the proteins were conjugated to pEGFP (Clonetech) or mCherry vector provided by Dr Roger Tsien (UCSD). Recombinant protein for kinesin light chain1 or mNUDC was generated using pGEX-4T expression vector (GE Healthcare Biosciences). Protein purification was performed using glutathione Sepharose 4B (GE Healthcare Biosciences) according to the manufacturer's recommendation. To remove GST tag, we treated recombinant protein with thrombin (Merck), followed by absorption of thrombin by benzamidine Sepharose 6B (GE Healthcare Biosciences).

DRG preparation, culture and fluorescence recovery measurement after photobleaching (FRAP)

The DRGs from post-natal mice were dissociated using a previously described method (Lindsay, 1988). During dissociation of cells, D-MEM was used with 10% heat-inactivated bovine serum, 200 ng/ml 2.5S mNGF (Sigma) and 5 μM uridine/deoxfluorouridine (Sigma). The cells were plated onto poly-D-lysine-coated dishes (MatTek) and cultured in the above medium for 48–72 h. The DRGs were transfected with vectors to express various proteins immediately after dissection using the Basic Nucleofector kit for primary neurons (Amaxa Biosystems). Fluorescence recovery measurement after photobleaching (FRAP) was carried out with an LSM 510 META confocal microscope (Carl Zeiss). Open box-shaped regions covering an axon were bleached 80–100 μm in length using the line-scan function at 488/405 nm, and recovery of fluorescence was monitored 10 μm in length at the proximal or distal side using the time-series function at 4-s intervals for up to 60 s. Anterograde flux was defined by the recovery of fluorescence at the proximal region, whereas retrograde flux was defined by the recovery at the distal region. A spacer region between two observatory areas ensured prevention of overlapping recovery from the opposite side.

For treatment with the blocking antibody, DRG neurons were permeabilized by 8 μM digitonin (Calbiochem) on ice for 1 min and washed with PBS containing 5% (w/v) bovine serum albumin (BSA; Wako), followed by administration of an anti-mNUDC antibody (8 mg/ml), an anti-$P150^{Glued}$ antibody (8 mg/ml) or an anti-dynamitin antibody (8 mg/ml). Observation of FRAP recovery was the same as described above. For the FRAP data of EGFP–$P150^{Glued}$ and EGFP–dynamitin, $t_{1/2}$ (s) was calculated using Origin Software (Microcal Software, Northhampton, MA).

Microtubule-binding assays

Purified kinesin from porcine brain was mixed with GST–NudC in the absence or presence of 10 mM ATP. The final concentration of kinesin was 35 μg/ml. The molar ratios of kinesin to NudC were 1:0, 1:1 and 1:3. MAP-depleted tubulin (0.4 mg/ml) and 50 μM taxol were added to the mixture, and then incubated for 5 min at room temperature. After kinesin binding, the microtubules were collected by centrifugation at 200 000 *g* for 10 min at room temperature using a 120.2 rotor in an Optima TLX ultracentrifuge (Beckman Coulter,

Fullerton, CA). The supernatants and pellets were separated and subjected to electrophoresis. The images of the gels were digitized and the bands were quantified by densitometry.

Microtubule-binding assays of mNudC

The MAP-depleted tubulin (0.8 mg/ml) was assembled in 50 μM taxol, then mixed with mNudC (8 μg/ml). Before mixture of mNudC, some of the samples were treated with kinesin (16 μg/ml). The microtubules and mNudC were incubated for 5 min at room temperature. After mNudC binding, microtubules were collected by centrifugation at 200 000 *g* for 10 min at room temperature using a 120.2 rotor in an Optima TLX ultracentrifuge (Beckman Coulter). The supernatants and pellets were separated and subjected to electrophoresis. After electrophoresis, proteins were transferred to PVDF membrane. The blots were probed with antibody raised against mNudC, followed by donkey anti-rabbit IgG conjugated to alkaline phosphatase. The blots were developed using the BCIP/NBT phosphatase substrate system.

Imaging of protein movements

For tracking mCherry– and EGFP–fused proteins in axons of DRG neurons from post-natal mice, an IX81 inverted microscope (Olympus) equipped with an FV-1000 confocal imaging system (Olympus) was used and controlled by MetaMorph software (MDS Analytical Technologies).

Generation of antibodies against mNUDC, P150^{Glued} and dynamitin

To make anti-mNUDC, P150^{Glued} or dynamitin antibodies, we immunized New Zealand white rabbits with a GST-conjugated recombinant mNUDC (70–200 AAs), P150^{Glued} (210–300 AAs) or dynamitin (1–230 AAs) expressed in bacteria and purified by GST–Sepharose (GE Healthcare) according to standard procedures. The antisera against mNUDC (70–200 AAs) protein, P150^{Glued} (210–300 AAs) protein or dynamitin (1–230 AAs) protein were collected, and purified by Hi-Trap NHS-activated HP columns (GE Healthcare) coupled with the antigens used, mNUDC (70–200 AAs), P150^{Glued} (210–300 AAs) or dynamitin (1–230 AAs).

siRNA preparation and transfection

Deprotected and double-stranded 21-nucleotide RNAs were synthesized by Japan Bio Service (Saitama, Japan) to target the mouse *mNudC* sequence, 5′-AACACCTTCTTCAGCTTCCTT-3′ as recommended in the study by Aumais *et al* (2003) (JCS). Firefly (*Photinus pyralis*) luciferase siRNA served as a negative control. siRNAs were re-suspended in RNase-free water at a final concentration of 20 μM and stored at −20°C until use. Mutated *mNudC* carrying 5′-AACACCTTCTTCAGTTTCCTT-3′ for rescue experiments was generated by QuickChange (Stratagene). EGFP-fused mutated *mNudC* was transfected for rescue experiments.

Immunocytochemistry

After 24 h, cells were fixed with 4% (w/v) ultra-pure electron microscopy-grade paraformaldehyde for 15 min at room temperature and permeabilized with 0.2% Triton X-100 for 5 min at room temperature. Cells were then blocked with 5% (w/v) BSA and Block Ace Powder (DS Pharma Biomedical) in PBS and incubated with anti-mNUDC, anti-LIS1, anti-DIC (Chemicon), anti-P150^{Glued}, anti-dynamitin, anti-β-COP (Sigma) and anti-EEA1 (Sigma) followed by incubation with Alexa546-conjugated anti-rabbit IgG (Molecular probes) or Alexa546-conjugated anti-mouse IgG (Molecular Probes). Each incubation was performed for 1 h at room temperature. Slides were mounted in ultra-pure electron microscopy-grade glycerine (Merck) containing 100 nM 4′, 6-diamidino-2-phenylindole (DAPI). Immunofluorescence analyses were examined with a laser scanning confocal microscope (TCS-SP5, Leica) and controlled by Photoshop software.

For detection of phenotypes after mNUDC depletion by siRNA, lysosomes and mitochondria were labelled by LysoTracker Green DND-26 (Molecular Probes) and pEYFP-Mito (Clonetech), respectively. Nucleus was labelled by Hoechst 33258 (Hoechst). For detection of clearer images, all images were captured in live conditions using the TCS-SP5 confocal microscope systems (Leica).

Sucrose gradient centrifugation and immunoprecipitation experiments

For sucrose gradient centrifugation experiments, 3×10^6 DRG neurons or 5×10^6 MEF cells transfected with fluorescence-tagged vector were cultured on poly-D-lysine-coated dish (BD Biocoat) and were collected and lysed in 1 ml of detergent-free PMEE buffer (35 mM PIPES (pH 7.2), 5 mM $MgSO_4$, 1 mM EGTA, 0.5 mM EDTA, 1 mM DTT and 0.5 mM ATP), followed by centrifugation for 5 min at 15 000 rpm at 4°C. About 600 μl of cell lysate was layered onto 4.2 ml of 15–30% linear sucrose gradient and centrifuged in a Hitachi P55ST2 swinging bucket rotor at 100 000 *g* for 16 h at 4°C. The sucrose gradients were fractionated into 15 300-ml fractions. Tyroglobulin (19.2 s), ferritin (16.5 s), catalase (11.2 s) and albumin (4.3 s) were used as markers. For immunoprecipitation experiments, DRG neurons were lysed in immunoprecipitation buffer (35 mM PIPES (pH 7.2), 5 mM $MgSO_4$, 1 mM EGTA, 0.5 mM EDTA, 1 mM DTT and 0.2% NP-40), followed by centrifugation for 3 min at 15 000 rpm at room temperature. Immunoprecipitation experiments were carried out from mouse brain extracts in using an anti-mNUDC rabbit polyclonal antibody, an anti-kinesin heavy chain antibody (H2, Chemicon) and an anti-dynein intermediate chain antibody (74.1, Chemicon) bound to protein G–Sepharose (GE Healthcare) in immunoprecipitation buffer for 1 h at room temperature. After five washes with the same immunoprecipitation buffer, bound proteins were eluted by boiling in SDS–PAGE sample buffer. The antibodies used are as follows: an anti-kinesin heavy chain antibody (H2, Chemicon), an anti-dynein intermediate chain antibody (74.1, Chemicon) and anti-P150^{Glued} mouse monoclonal antibody (BD Bioscience). For immunoabsorption, mouse brain extracts were incubated with 25 μg anti-mNUDC antibody, anti-P150^{Glued} antibody or anti-dynamitin antibody, which had been conjugated with protein-A or protein-G Sepharose (GE Healthcare), at room temperature for 1 h. Supernatant was further subjected to immunoprecipitation analysis.

In vitro motility assay

The previously described *in vitro* motility assay (Yamada *et al*, 2008) was modified for transportable microtuble (tMT) or dynactins. A coverslip (18 × 18 mm; Matsunami Glass) was placed on the center of another coverslip (24 × 42 mm; Matsunami Glass) using two strips of double-coated tape to make a flow chamber. Kinesin (Wagner *et al*, 1991), dynactins (Bingham *et al*, 1998) and tubulin (Vallee, 1986) were purified from fresh porcine brain as reported previously, with some modification. The tubulin was labelled with Cy3 mono-Reactive Dye Pack (GE Healthcare), Cy5 mono-Reactive Dye Pack (GE Healthcare) or FluoReporter Tetramethyrhodamine Protein Labeling Kit (Invitrogen). Fluorescent MTs were prepared by co-polymerization of labelled and unlabelled tubulin at a molar ratio of 1:100 and 1:750 for FL-labelled transportable MT and FL-labelled rail MT, respectively. For assays, MTs with a length of 2–5 μm as tMTs and with a length of 20–50 μm as rail MTs were prepared. Polymerization was performed in BRB80 buffer (80 mM PIPES (pH 6.8), 1 mM $MgCl_2$, 1 mM EGTA) containing 6 mM GTP at 37°C for 30 min and 33 μM Taxol (Sigma) was added to maintain the polymerization. The dynactin complex was eluted from the Hi-Trap Q column (GE Healthcare) with approximately 250 mM KCl (Toba and Toyoshima, 2004) and labelled with Cy3, Cy5 or TMRA. First, anti-α tubulin (0.5 mg/ml, TU-02, Santa Cruz Biotechnology) was introduced into the observation chamber and absorbed onto the glass for 10 min. The following were then added in sequence: (1) 5 mg/ml BSA in BRB80 buffer to remove unabsorbed the antibody and to block the glass surface for 2 min. (2) 20–30 μg/ml of FL MT in BRB80 buffer containing 1 mM ATP, 33 μM Taxol and an oxygen scavenger (4.5 mM glucose, 216 μg/ml glucose oxidase, 36 μg/ml catalase, 1% 2-mercaptoethanol) as the 'rail MTs' for 20 min. (3) 5 mg/ml BSA in BRB80 buffer to remove unabsorbed the antibody and to further block the glass surface for 5 min. (4) FL-labelled tMT (transportable MTs, 30 μg/ml) or FL-labelled dynactin (0.2–0.3 mg/ml), kinesin (2–5 μg/ml), GST–mNUDC (60–80 μg/ml) and pre-immune rabbit serum (400 μg/ml) or anti-mNUDC (400 μg/ml) were pre-incubated at 37°C for 5 min and then introduced into the chamber. Fluorescent MTs and dynactins were imaged using a conventional inverted fluorescence microscope (ECLIPSE TE2000-U, Nikon) with an oil-immersion objective lens (Plan Apo TIRF, × 100, NA = 1.45, Nikon) and analysed by Andor SOLIS (Andor technology).

Supplementary data
Supplementary data are available at *The EMBO Journal* Online (http://www.embojournal.org).

Acknowledgements

We thank Yoshihiko Funae, Hiroshi Iwao, Toshio Yamauchi, Masami Muramatsu, Yoshitaka Nagai and Michiyuki Matsuda for generous support and encouragement. We also thank Tomotaka Komori and Masatoshi Morimatsu for technical support. This study was supported by Grant-in-Aid for Scientific Research from the Ministry of Education, Science, Sports and Culture of Japan from the Ministry of Education, Science, Sports and Culture of Japan to SH; by The Mother and Child Health Foundation, The Naito Foundation, Japan Brain Foundation and The Uehara Memorial Foundation to SH, and NIH grants NS41030 and HD47380 to AW-B.

Conflict of interest

The authors declare that they have no conflict of interest.

References

Aumais JP, Tunstead JR, McNeil RS, Schaar BT, McConnell SK, Lin SH, Clark GD, Yu-Lee LY (2001) NudC associates with Lis1 and the dynein motor at the leading pole of neurons. *J Neurosci* **21:** RC187

Aumais JP, Williams SN, Luo W, Nishino M, Caldwell KA, Caldwell GA, Lin SH, Yu-Lee LY (2003) Role for NudC, a dynein-associated nuclear movement protein, in mitosis and cytokinesis. *J Cell Sci* **116:** 1991–2003

Bingham JB, King SJ, Schroer TA (1998) Purification of dynactin and dynein from brain tissue. *Methods Enzymol* **298:** 171–184

Dobyns WB, Reiner O, Carrozzo R, Ledbetter DH (1993) Lissencephaly. A human brain malformation associated with deletion of the LIS1 gene located at chromosome 17p13. *JAMA* **270:** 2838–2842

Dobyns WB (1989) The neurogenetics of lissencephaly. *Neurol Clin* **7:** 89–105

Echeverri CJ, Paschal BM, Vaughan KT, Vallee RB (1996) Molecular characterization of the 50-kD subunit of dynactin reveals function for the complex in chromosome alignment and spindle organization during mitosis. *J Cell Biol* **132:** 617–633

Eckley DM, Gill SR, Melkonian KA, Bingham JB, Goodson HV, Heuser JE, Schroer TA (1999) Analysis of dynactin subcomplexes reveals a novel actin-related protein associated with the arp1 minifilament pointed end. *J Cell Biol* **147:** 307–320

Efimov VP, Morris NR (2000) The LIS1-related NUDF protein of *Aspergillus nidulans* interacts with the coiled-coil domain of the NUDE/RO11 protein. *J Cell Biol* **150:** 681–688

Faulkner NE, Dujardin DL, Tai CY, Vaughan KT, O'Connell CB, Wang Y, Vallee RB (2000) A role for the lissencephaly gene *LIS1* in mitosis and cytoplasmic dynein function. *Nat Cell Biol* **2:** 784–791

Gindhart Jr JG, Desai CJ, Beushausen S, Zinn K, Goldstein LS (1998) Kinesin light chains are essential for axonal transport in *Drosophila*. *J Cell Biol* **141:** 443–454

Gupta A, Tsai LH, Wynshaw-Boris A (2002) Life is a journey: a genetic look at neocortical development. *Nat Rev Genet* **3:** 342–355

Hackney DD, Levitt JD, Suhan J (1992) Kinesin undergoes a 9 S to 6 S conformational transition. *J Biol Chem* **267:** 8696–8701

Han G, Liu B, Zhang J, Zuo W, Morris NR, Xiang X (2001) The *Aspergillus* cytoplasmic dynein heavy chain and NUDF localize to microtubule ends and affect microtubule dynamics. *Curr Biol* **11:** 719–724

Holleran EA, Karki S, Holzbaur EL (1998) The role of the dynactin complex in intracellular motility. *Int Rev Cytol* **182:** 69–109

Kuznetsov SA, Gelfand VI (1986) Bovine brain kinesin is a microtubule-activated ATPase. *Proc Natl Acad Sci USA* **83:** 8530–8534

Ligon LA, Tokito M, Finklestein JM, Grossman FE, Holzbaur EL (2004) A direct interaction between cytoplasmic dynein and kinesin I may coordinate motor activity. *J Biol Chem* **279:** 19201–19208

Lindsay RM (1988) Nerve growth factors (NGF, BDNF) enhance axonal regeneration but are not required for survival of adult sensory neurons. *J Neurosci* **8:** 2394–2405

Minke PF, Lee IH, Tinsley JH, Bruno KS, Plamann M (1999) *Neurospora crassa ro-10* and *ro-11* genes encode novel proteins required for nuclear distribution. *Mol Microbiol* **32:** 1065–1076

Mori D, Yamada M, Mimori-Kiyosue Y, Shirai Y, Suzuki A, Ohno S, Saya H, Wynshaw-Boris A, Hirotsune S (2009) An essential role of the aPKC–Aurora A–NDEL1 pathway on neurite elongation by modulation of microtubule dynamics. *Nat Cell Biol* **11:** 1057–1068

Morris NR, Efimov VP, Xiang X (1998a) Nuclear migration, nucleokinesis and lissencephaly. *Trends Cell Biol* **8:** 467–470

Morris SM, Albrecht U, Reiner O, Eichele G, Yu-Lee LY (1998b) The lissencephaly gene product Lis1, a protein involved in neuronal migration, interacts with a nuclear movement protein, NudC. *Curr Biol* **8:** 603–606

Niethammer M, Smith DS, Ayala R, Peng J, Ko J, Lee MS, Morabito M, Tsai LH (2000) NUDEL is a novel Cdk5 substrate that associates with LIS1 and cytoplasmic dynein. *Neuron* **28:** 697–711

Rahman A, Kamal A, Roberts EA, Goldstein LS (1999) Defective kinesin heavy chain behavior in mouse kinesin light chain mutants. *J Cell Biol* **146:** 1277–1288

Reiner O, Carrozzo R, Shen Y, Wehnert M, Faustinella F, Dobyns WB, Caskey CT, Ledbetter DH (1993) Isolation of a Miller–Dieker lissencephaly gene containing G protein beta-subunit-like repeats. *Nature* **364:** 717–721

Sasaki S, Shionoya A, Ishida M, Gambello MJ, Yingling J, Wynshaw-Boris A, Hirotsune S (2000) A LIS1/NUDEL/cytoplasmic dynein heavy chain complex in the developing and adult nervous system. *Neuron* **28:** 681–696

Schroer TA (2004) Dynactin. *Annu Rev Cell Dev Biol* **20:** 759–779

Smith DS, Niethammer M, Ayala R, Zhou Y, Gambello MJ, Wynshaw-Boris A, Tsai LH (2000) Regulation of cytoplasmic dynein behaviour and microtubule organization by mammalian Lis1. *Nat Cell Biol* **2:** 767–775

Stock MF, Guerrero J, Cobb B, Eggers CT, Huang TG, Li X, Hackney DD (1999) Formation of the compact confomer of kinesin requires a COOH-terminal heavy chain domain and inhibits microtubule-stimulated ATPase activity. *J Biol Chem* **274:** 14617–14623

Toba S, Toyoshima Y-Y (2004) Dissociation of double-headed cytoplasmic dynein into single-headed species and its motile properties. *Cell Motil Cytoskeleton* **58:** 281–289

Toyo-oka K, Shionoya A, Gambello MJ, Cardoso C, Leventer R, Ward HL, Ayala R, Tsai LH, Dobyns W, Ledbetter D, Hirotsune S, Wynshaw-Boris A (2003) 14-3-3epsilon is important for neuronal migration by binding to NUDEL: a molecular explanation for Miller–Dieker syndrome. *Nat Genet* **34:** 274–285

Vale RD, Reese TS, Sheetz MP (1985a) Identification of a novel force-generating protein, kinesin, involved in microtubule-based motility. *Cell* **42:** 39–50

Vale RD, Schnapp BJ, Mitchison T, Steuer E, Reese TS, Sheetz MP (1985b) Different axoplasmic proteins generate movement in opposite directions along microtubules *in vitro*. *Cell* **43:** 623–632

Vallee RB, Tai C, Faulkner NE (2001) LIS1: cellular function of a disease-causing gene. *Trends Cell Biol* **11:** 155–160

Vallee RB, Tsai JW (2006) The cellular roles of the lissencephaly gene *LIS1*, and what they tell us about brain development. *Genes Dev* **20:** 1384–1393

Vallee RB (1986) Reversible assembly purification of microtubules without assembly-promoting agents and further purification of tubulin, microtubule-associated proteins, and MAP fragments. *Methods Enzymol* **134:** 89–104

Wagner MC, Pfister KK, Brady ST, Bloom GS (1991) Purification of kinesin from bovine brain and assay of microtubule-stimulated ATPase activity. *Methods Enzymol* **196:** 157–175

Wynshaw-Boris A (2007) Lissencephaly and LIS1: insights into the molecular mechanisms of neuronal migration and development. *Clin Genet* **72:** 296–304

Xiang X, Osmani AH, Osmani SA, Xin M, Morris NR (1995) *NudF*, a nuclear migration gene in *Aspergillus nidulans*, is similar to the human *LIS-1* gene required for neuronal migration. *Mol Biol Cell* **6:** 297–310

Xiang X, Zuo W, Efimov VP, Morris NR (1999) Isolation of a new set of *Aspergillus nidulans* mutants defective in nuclear migration. *Curr Genet* **35:** 626–630

Yamada M, Toba S, Yoshida Y, Haratani K, Mori D, Yano Y, Mimori-Kiyosue Y, Nakamura T, Itoh K, Fushiki S, Setou M, Wynshaw-Boris A, Torisawa T, Toyoshima YY, Hirotsune S (2008) LIS1 and NDEL1 coordinate the plus-end-directed transport of cytoplasmic dynein. *EMBO J* **27:** 2471–2483

Yamada M, Yoshida Y, Mori D, Takitoh T, Kengaku M, Umeshima H, Takao K, Miyakawa T, Sato M, Sorimachi H, Wynshaw-Boris A, Hirotsune S (2009) Inhibition of calpain increases LIS1 expression and partially rescues *in vivo* phenotypes in a mouse model of lissencephaly. *Nat Med* **15:** 1202–1207

Yingling J, Youn YH, Darling D, Toyo-Oka K, Pramparo T, Hirotsune S, Wynshaw-Boris A (2008) Neuroepithelial stem cell proliferation requires LIS1 for precise spindle orientation and symmetric division. *Cell* **132:** 474–486

Zhang J, Li S, Fischer R, Xiang X (2003) Accumulation of cytoplasmic dynein and dynactin at microtubule plus ends in *Aspergillus nidulans* is kinesin dependent. *Mol Biol Cell* **14:** 1479–1488

Zhou T, Zimmerman W, Liu X, Erikson RL (2006) A mammalian NudC-like protein essential for dynein stability and cell viability. *Proc Natl Acad Sci USA* **103:** 9039–9044

Zhuang L, Zhang J, Xiang X (2007) Point mutations in the stem region and the fourth AAA domain of cytoplasmic dynein heavy chain partially suppress the phenotype of NUDF/LIS1 loss in *Aspergillus nidulans*. *Genetics* **175:** 1185–1196